NONLINEAR ANALYSIS OF EDDY-CURRENT COUPLINGS IN FEEDBACK CONTROL SYSTEMS

by

Eric Theodore Carlen

Thesis submitted to the Graduate Faculty of the
Virginia Polytechnic Institute
in candidacy for the degree of

MASTER OF SCIENCE

in

Electrical Engineering

APPROVED:

Chairman, Dr. M. H. Hopkins, E. E. Dept.

Dr. R. H. Miller, E. E. Dept.

Professor R. R. Wright, E. E. Dept.

Professor E. A. Manus, E. E. Dept.

May 1966

Blacksburg, Virginia

II. TABLE OF CONTENTS

		Page
I.	TITLE PAGE	1
II.	TABLE OF CONTENTS	2
	A) List of Figures	3
	B) List of Symbols	4
III.	INTRODUCTION	5
	A) General Description	8
IV.	REVIEW OF LITERATURE	10
V.	THE INVESTIGATION	17
	A) Object of the Investigation	17
	B) Equipment Used in the Investigation	17
	C) Description of the System	17
	D) Analysis of the System	19
	1) System Equations	19
	2) Block Diagram Simplification	19
	3) Field Current Loop	21
	4) Velocity Loop	24
	5) Describing Function Development	27
	6) Stability Analysis With the Gain-Phase Shift Plot	33
	7) Analog Computer Simulation	36
VI.	DISCUSSION OF THE RESULTS	38
VII.	SUMMARY AND CONCLUSIONS	47
VIII.	ACKNOWLEDGMENTS	49
IX.	BIBLIOGRAPHY	50
	A) Literature Cited	50
	B) Literature Examined	51
X.	VITA	52

List of Figures

Figure		Page
1	Basic Eddy-Current Coupling	8
2	Speed-Torque Function	12
3	Machine Configuration	15
4	Machine Characteristics	16
5	System Block Diagram	20
6	Field Current Loop Block Diagram	21
7	Field Current Gain-Frequency Plot	23
8	Reduced Block Diagram	24
9	Speed Loop Gain-Frequency Plot	26
10	Describing Function Illustration	28
11	Describing Function Plot	32
12a	Nichol's Chart Overlay	34
12b	Speed Loop Gain-Phase Shift Plot	35
13	Nonlinear Compensation Scheme	37
14	Compensation Effects	39
15	Nonlinear System Speed Response (High Gain)	41
16	Nonlinear System Speed Response (Low Gain)	42
17	Brearley Approximation and Computer Comparison	43
18	Linear System Speed Response (High and Low Gain)	44
19	Speed Response at Various Torque Load Levels With Nonlinear Compensation	45
20	Analog Computer Diagrams	46

List of Symbols

A - Amplitude of signal input to the describing function

α - Acceleration rpm/sec

C - Controlled variable

E_f - Composite Eddy-Current Coupling field voltage

FRS - Field Dropping Resistor Ohms

G - Forward Gain

G_D - Describing Function

H - Feedback Gain

I_f - Field Current amperes

I_1 - Field Current Bias

J - Total System Inertia lb-ft/rpm/sec

K_1 - Speed Amplifier Gain

K2 - Field Current Amplifier Gain

K3 - Speed-Torque Characteristic

K_{Tach} - Tachometer Gain

M_m - Maximum Closed Loop Magnitude

N - Speed rpm

R_f - Field Resistance Ohms

T_f - Field Time Constant

T_1 - Speed Loop Lead Compensation Time Constant

T_2 - Power Amplifier Time Constant

T_3 - Field Current Loop Lead Time Constant

τ - Torque

τ_D - Torque Developed

τ_L - Torque Load

t_r - Rise Time 10% to 90% final value

t_s - Settling Time to stay within 5% final value

ω - Angular Frequency

III. INTRODUCTION

During the latter part of 1961, the author was engaged in the design of four eddy-current-coupling dynamometer drives for the Socony Mobile Research Laboratory. The drive systems were in the 400 to 600 horsepower range having field current and speed regulation. The specified performance required the maximum attainable from present state-of-the-art hardware. At that time, however, an accurate transfer function for the eddy-current coupling did not exist. A linearized analysis was made and an analog computer simulation was performed using a model developed by H. Gibson[1] of the General Electric Company, Schenectady, New York. The final design based on this simulation yielded installed system results that were in close agreement with those predicted by the computer study. Since that time this model has been used with a great deal of success in the design of eddy-current coupling drive systems and also in the prediction of drive performance.

Eddy-current couplings have wide application in control systems, ranging from industrial processes to radar antenna drives. The low cost in the former application, and high response in the latter are outstanding features of this device. The absence of both exposed rotating windings and a commutator allows operation at speeds up to 20,000 rpm.

In turbine testing, where high speed power absorption is required, a special form of eddy-current coupling is used where the inductor is cradled and coupled to a scale or load cell. Drum losses are dissipated by circulating cooling air or water in the gap between the inductor and loss drum.

The eddy-current coupling described in this thesis has not yet been built, but the specifications are realistic and the design is similar to those provided for antenna drives. Two couplings are used to provide a full reversing drive as shown in Figure 3.

Although many eddy-current couplings have been designed and put into service, the development of a straightforward design procedure has been missing. The usual method of attack has been to restrict operation to small excursions about an operating point so that a linear analysis could be used. In this paper, a transfer function is developed from the work of E. J. Davies[2] and applied to an analysis of the full reversing eddy-current coupling drive. This analysis will include a derivation of the system equations; derivation of a suitable describing function; a solution to the non-linear equations by the describing function method; and an analog computer study, with a discussion of the various compensation techniques.

General Description

The eddy-current coupling is an electrical clutch capable of controlling torque transfer from motor to machine.

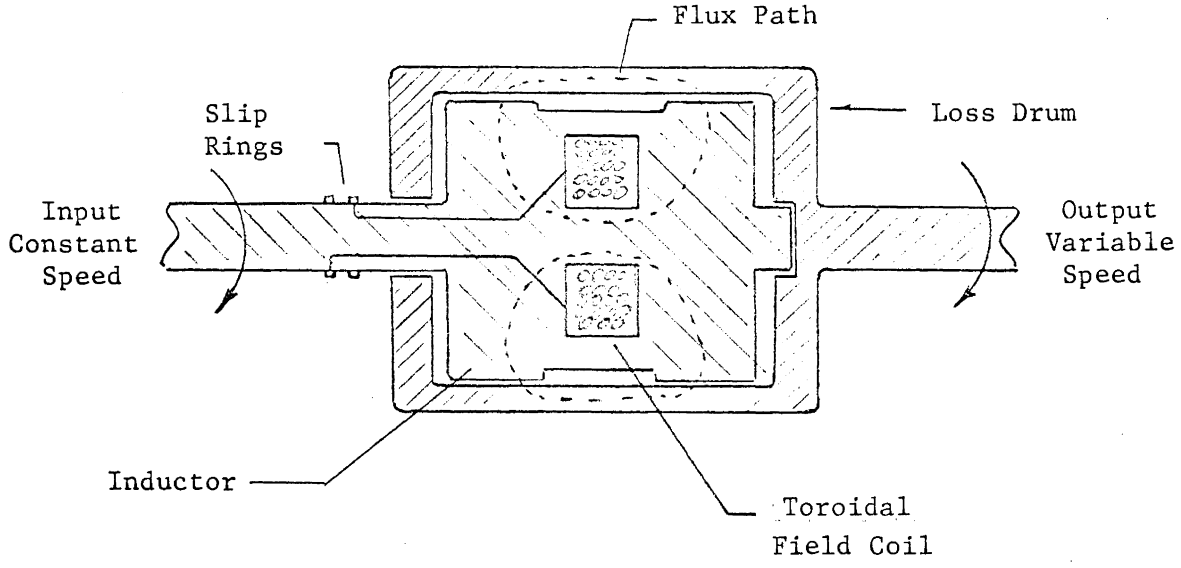

Figure 1

The input shaft is driven by a motor at constant speed. A torroidal field coil is excited by direct current. As the inductor rotates, relative to the loss drum, a variation in air gap flux density occurs as a result of teeth machined on the inductor gap surface. The variation in air gap flux density produces eddy currents in the loss drum. The eddy currents in the loss drum then produce torque on the output shaft. Power transfer from the input shaft to the output shaft can be expressed in terms of their relative speed.

$$\text{Output Power} = \frac{1-S}{S} \quad [\text{Drum Loss}]$$

$$\text{Slip} \qquad S = \frac{\text{Relative Speed}}{\text{Input Speed}}$$

The above equations point out the fact that the eddy-current coupling is inefficient when operating at high slip speeds. Another feature which may be a desirable or undesirable feature depending upon the application is the nonlinear relation between torque and field current, $\tau = I_f^2$. An introduction to this problem is presented with the following example: A unit step is applied to a first order lag, the output of which is then squared.

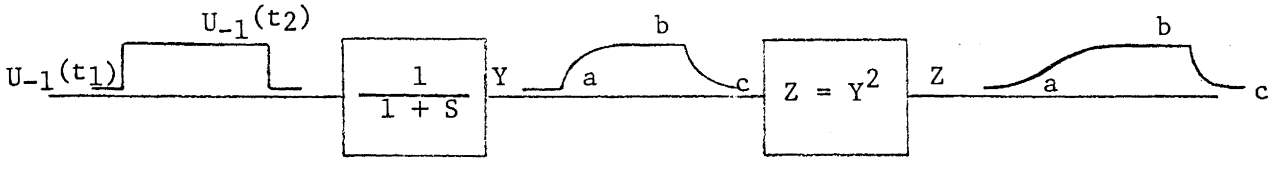

$$Y_{a\to b} = 1-e^{-t}$$

$$Y_{b\to c} = e^{-t}$$

$$Z_{a\to b} = 1-2e^{-t} + e^{-2t}$$

$$Z_{b\to c} = e^{-2t}$$

The time response at Z in the on direction contains two time constants T = 1 sec. and T' = 1/2 sec. The time response in the off direction contains only the one time constant T' = 1/2 sec. It will be shown subsequently that this feature enhances performance when compared to an equivalent linear system. On the other hand, the nonlinearity is shown to be undesirable when steady-state torque loading is introduced to the system.

IV. THE REVIEW OF LITERATURE

The general equations that are used to describe the eddy-current coupling in terms of torque vs. field current and speed vs. torque are taken from "A Study of the Fully-Interdigitated Eddy-Current Coupling"[2] by E. John Davies. This was the topic of his doctoral thesis. His work is the latest and most comprehensive study of the eddy-current coupling which builds upon earlier work done by Rudenberg[3], Dunaevski[4] and Gibbs[5]. The general equations are stated as follows.

1. Variation of torque with field current

$$I_f = C_1 \frac{\tau^{0.35}}{N^{0.325}} + C_2 \frac{\tau^{0.65}}{N^{0.325}}$$

At constant speed this becomes:

$$I_f = C_3\tau^{0.35} + C_4\tau^{0.65}$$

When the slip speed is large,

$$\tau = I_f^{1.54}$$

When the slip speed is low;

$$\tau = I_f^{2.85}$$

The following approximate relationship will be used in this analysis which holds over a wide range of slip speeds.

$$\tau = I_f^{2}$$

2. Variation of torque with speed

$$\tau/\tau_M = \frac{4\,(N/N_m)^{0.65}\,(\tau/\tau_M)^{0.3}}{[1 + (N/N_m)^{0.65}\,(\tau/\tau_m)^{0.3}]^2}$$

Where τ_M = maximum rated torque

N_M = speed at which τ_M occurs

A plot of this equation is shown in Figure 2. An important relationship used in the development of the above equations is the equation for total excitation, Ag, supplied to the air gap.

$$Ag = C1\,\frac{\tau^{0.35}}{N^{0.325}} + C2\tau^{0.65}\,N^{0.325}$$

The first quantity on the right hand side of the equation is the fundamental flux per pole while the second quantity is armature reaction. From this equation it can be seen that a transient in torque or speed will affect total airgap excitation with respect to time which, of course, will be reflected in the field circuit. Experimental data taken by W. K. Volkman[6] shows the effect of a large change in speed at the rate of 1000 rpm/sec. on field current and torque. The peak transient change in torque amounted to approximately 12% of rated torque. This effect is not included in this analysis due to its relatively small magnitude and also because the added complexity of the analysis would not justify the additional work.

Other effects which have not been included in this analysis are those due to eddy-current time constants. These originate from closed

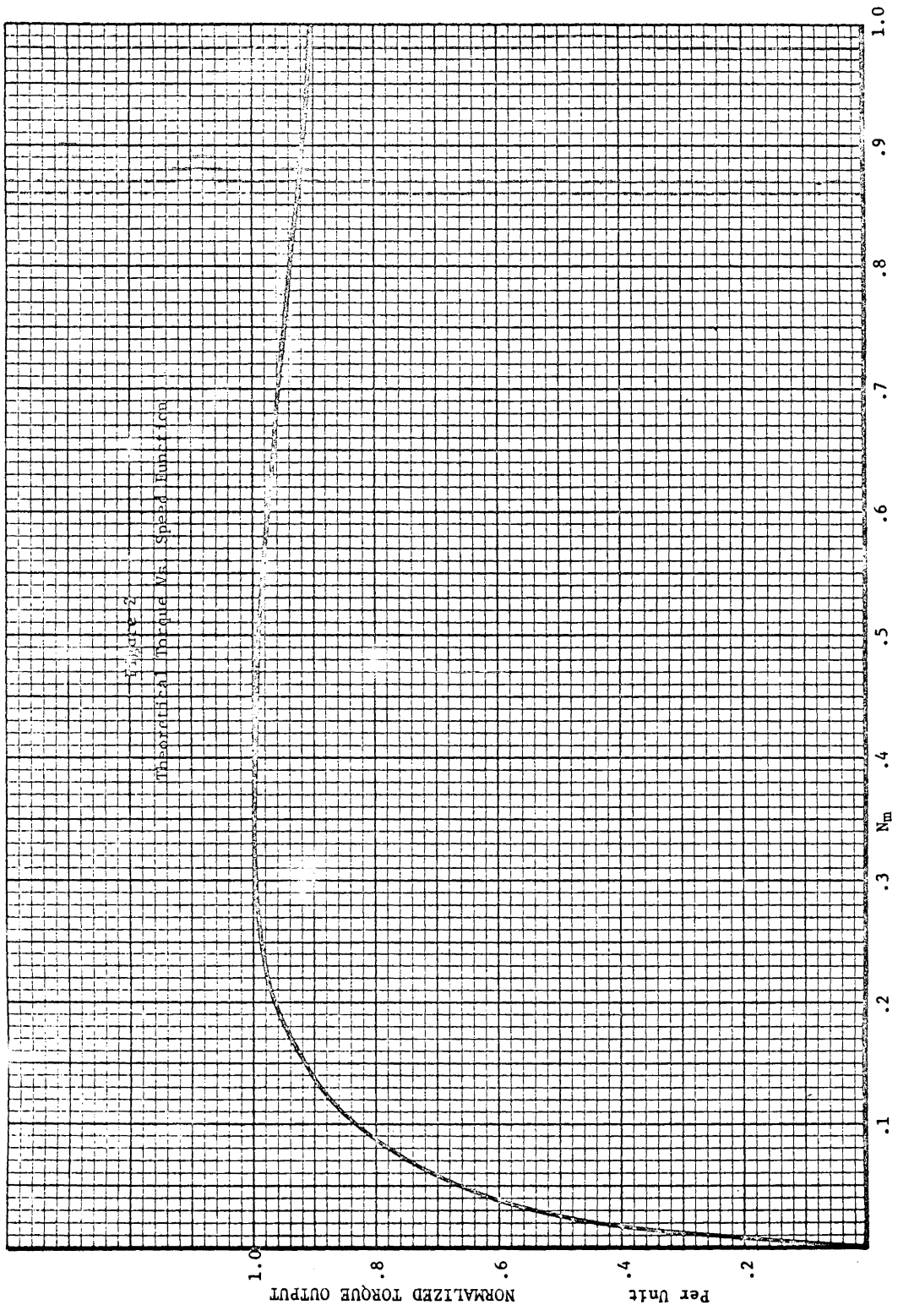
Figure 2
Theoretical Torque Vs. Speed Function
NORMALIZED TORQUE OUTPUT
Per Unit
1.0
.8
.6
.4
.2
.1
.2
.3
.4
.5
.6
.7
.8
.9
1.0
SLIP
N_m

Figure 2

current paths in the stator and rotor which have inductive and resistive parameters that are not readily calculated.

The transfer function from field voltage to current for a linear R-L circuit is:

$$\frac{I_f}{E_f} = \frac{1/R_f}{1 + T_f S} \qquad \text{where } T_f = \frac{L_f}{R_f}$$

In the presence of eddy currents, frequency response tests performed by H. Gibson[1] show the transfer function to be of the following form:

$$\frac{I_f}{E_f} = \frac{1/R_f \ (1 + T_1 S) \ (1 + T_3 S)}{(1 + T_f S) \ (1 + T_2 S) \ (1 + T_4 S)}$$

where $T_f > T_1 > T_2 > T_3 > T_4$

Since the eddy-current coupling is normally used in speed and position regulators, the time constants due to eddy currents will be sufficiently beyond unity gain crossover and therefore have a minor effect. The most serious problem, however, is that there is no way of readily forcing eddy-current time constants. Forcing is used here to mean the placing of additional resistance in series with the inductance or adding gain and applying excessive voltage transiently under negative feedback to increase the rate of change of current, thereby reducing the time constant. This aspect puts a limit on the amount of effective forcing of the field time constant which is usually in the order of between three-to-one and six-to-one, depending on machine parameters. The foregoing discussion applies not only to eddy-current couplings but to all solid frame machines such as D-C generators and motors.

The transfer function, I_f/E_f, used in this analysis does not include any effects due to saturation since heavy saturation is not encountered over the normal operating range of the eddy current coupling.

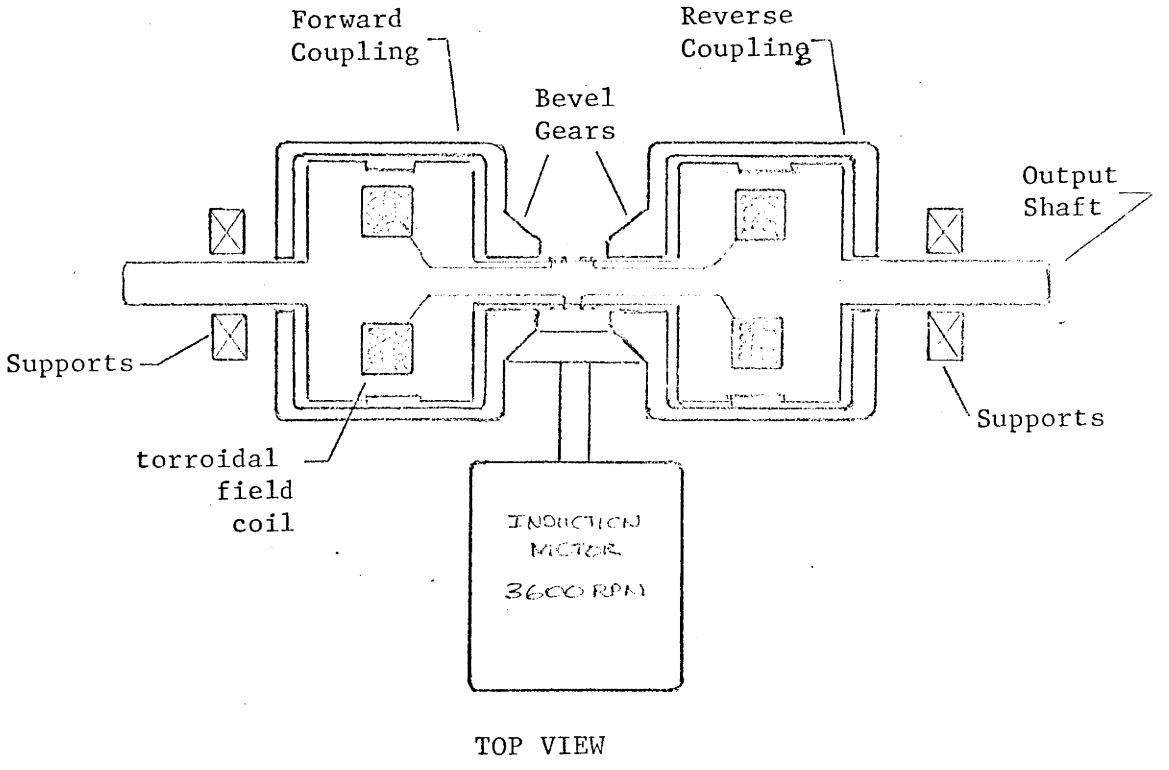

Figure 3. Full-Reversing Eddy-Current Coupline Drive

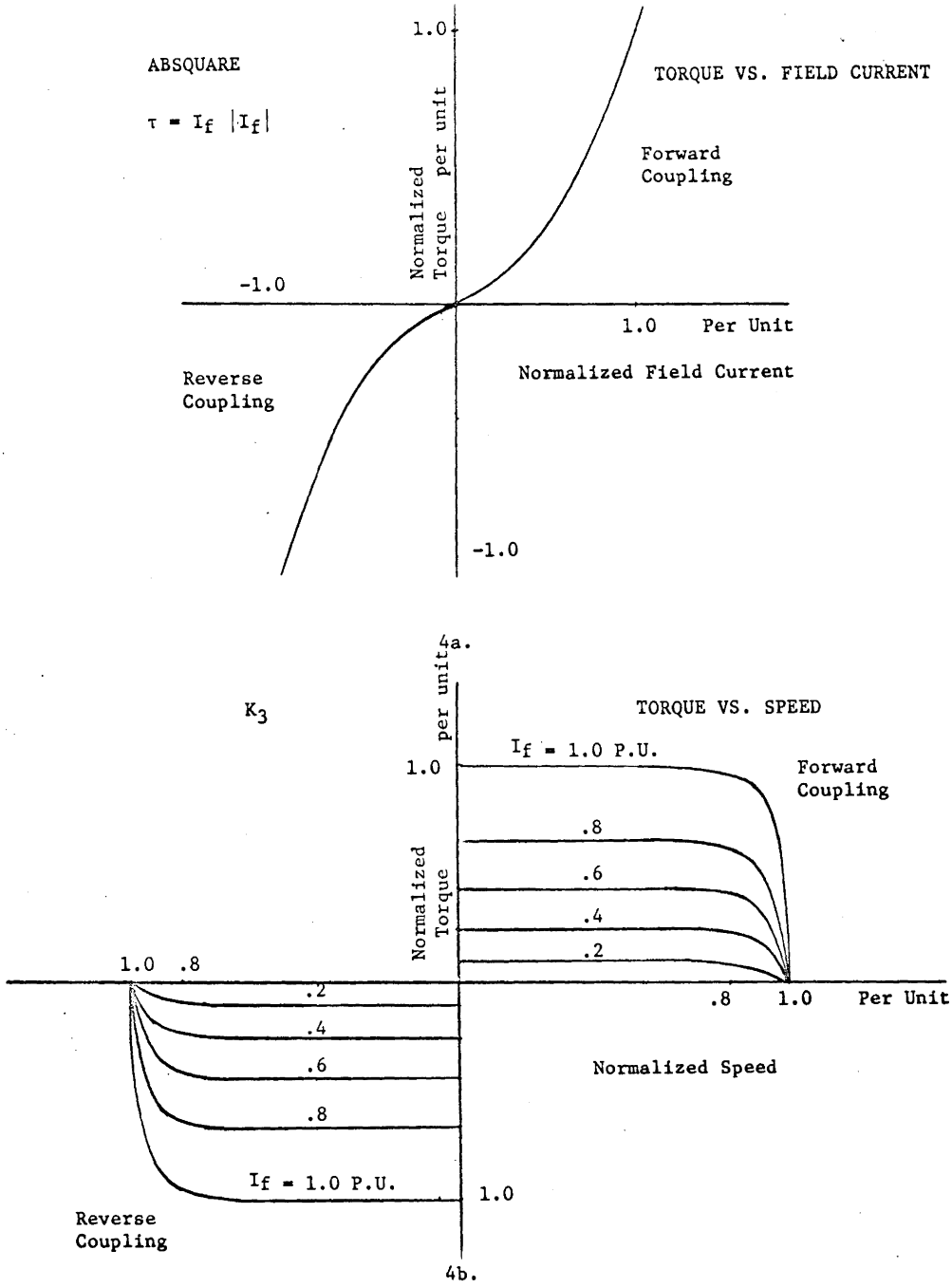

Figure 4. Machine Characteristics

V. THE INVESTIGATION

A. Object of the Investigation

The fundamental aim is to develop a readily usable analytical approach to the design of control systems with eddy-current couplings. Other objectives are to compare the nonlinear response with an equivalent linear response and also to develop a means of compensation where linear response is required.

B. Equipment Used in the Investigation

The Pace TR-48 analog computer manufactured by Electronic Associates Inc. was used in the computer simulation. Readout equipment available on this computer and used in the simulation is listed as follows:

a. EAI X-Y Plotter Model 1110

b. EAI Digital Voltmeter

c. EAI 4-Channel Oscilloscope

C. System Description

Figure 3 best illustrates the machine layout while figures 2 and 4 describe some of the more important characteristics of the eddy-current coupling. The system used in this investigation is of the full reversing type having two couplings arranged in a push-pull configuration.

a. Power Amplifiers

Maximum Output Voltage	180V DC
Maximum Output Power	5 KW
Maximum Output Current	50 Amperes
Input Supply Voltage	220V AC
Gain	10 V/V
Bandwidth	500 cps

b. Eddy-Current Couplings

Maximum Dissipation	50 HP
Maximum Torque	62.5 lb-ft
Maximum Speed	20,000 rpm (20,000 rpm = 1 p.u.)
Total Drive Inertia, J	.33 lb-ft-sec^2
Field Resistance R_f	1.25 Ohms
Maximum Field Current I_f max.	40 Amperes
Field Time Constant T_f	.1 Seconds

c. Induction Drive Motor

Power Rating	60 HP
Speed	3600 rpm
Gear Ratio	6:1
Input Power	440V AC 3PH

d. Tachometer

Type	DC Homopolar
Gain	100 ma/1000 rpm

D. Analysis of the System

1. System Equations

$$\tau_{developed} - \tau_{load} = \tau_{acceleration} = J\alpha$$

$$\alpha = \frac{1}{J} (\tau_d - \tau_L)$$

$$N_{shaft} = \frac{1}{S} \text{ X } \alpha = \frac{1}{JS} (\tau_d - \tau_L)$$

$$\tau_{developed} = K_3 N_{shaft} \tau$$

$$\tau = I_f |I_f|$$

$$I_f = \frac{1/R_f}{1 + T_f S} E_f$$

Field current feedback voltage = I_f X FRS

Speed feedback = K_{tach} X N_{shaft}

The preceding equations are presented in block diagram form, Figure 5.

2. Block Diagram Simplification

The block diagram of Figure 5 can be simplified after an examination of gain element K_3. Refer to Figure 4 page 16. Over the useful operating speed range (0 to .8 p.u.);

$$dT/dN \simeq 0$$

$$T \simeq 1.0$$

Then, $T_{developed} = T$

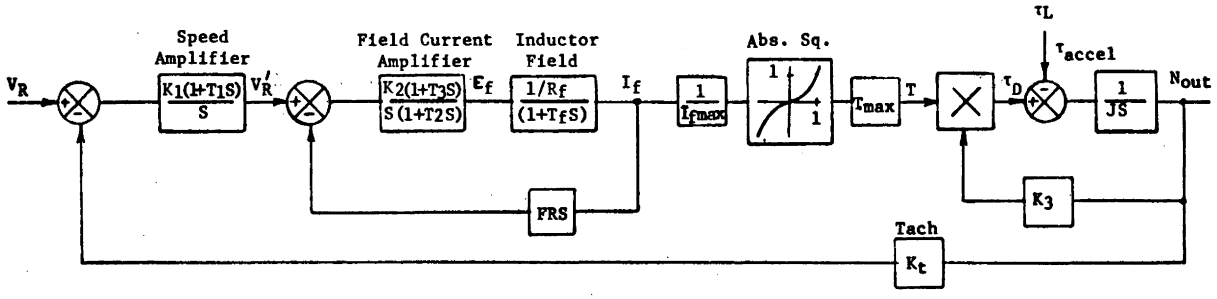

Figure 5. Block Diagram

FRS - Field Dropping Resistor

I_f - Field Current

J - Total System Inertia

K_1 - Speed Amplifier Gain

K_2 - Field Current Amplifier Gain

K_3 - Speed Torque Characteristic

K_t - Tachometer Gain

N_{out} - Output Shaft Speed

R_f - Field Resistance

T_f - Field Time Constant

T_1 - Speed Loop Lead Compensation

T_2 - Power Amplifier Lag

T_3 - Current Loop Lead

τ - Torque

τ_D - Torque Developed

τ_L - Torque Load

E_f - Field Voltage

V_R - Speed Loop Reference

V_R' - Current Loop Reference

3. Field Current Loop

The field current loop as taken from the block diagram, Figure 5, is shown below:

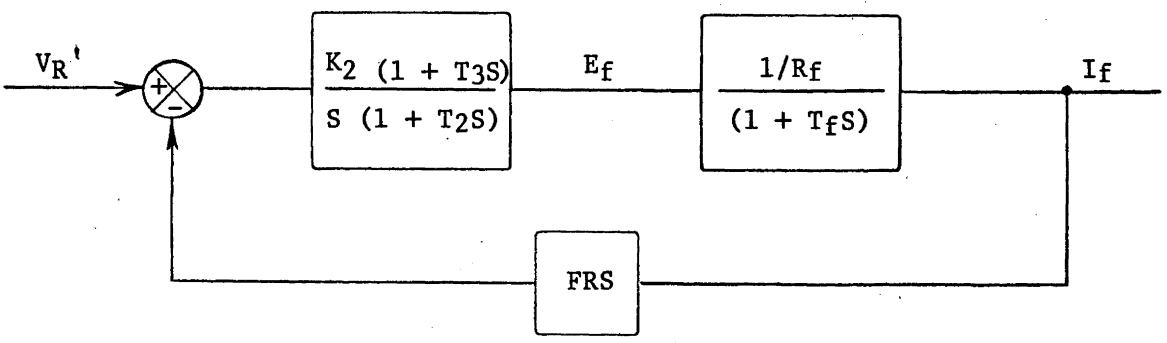

Figure 6

This field current loop is a composite loop since in the actual system of Figure 3 there are two couplings. hence two fields and two power amplifiers to drive the fields. However, since operation is push-pull, without magnetic coupling, the field current loops operate independently on either side of zero, with the exception of a small amount of overlap. This being the case, a single composite loop may be used for design analysis purposes. Let $T_3 = T_f$ for 20db/decade attenuation in the vicinity of unity gain cross-over. With a limit on forcing ratio of 3 to 1 as discussed in the introduction and a field time constant of .1 seconds,

closed loop bandwidth has an upper limit of 30 rad/sec before power amplifier saturation takes place on a full scale output swing.

$$\omega_{b.w.} = \frac{1}{.1 \text{ secs.}/3} = 30 \text{ rad/sec. for } T_f >> T_2$$

The required amount of feedback gain is based on a full-scale reference voltage of 20 volts and a full-scale field current of 40 amps at zero frequency.

$$\left|\frac{If}{V_R'}\right|_{\omega = 0} = \frac{1}{H} = \frac{40 \text{ amps}}{20 \text{ volts}} = 2 \qquad H = .5 \frac{\text{volts}}{\text{amps}}$$

The forward gain and the inverse of feedback gain are plotted in Figure 7. The forward gain, G, is positioned so that the intersection with the inverse feedback gain, $\frac{1}{H}$, occurs at 30 rad/sec. The curve obtained by following $\frac{1}{H}$ before the intersection and G after the intersection is the closed loop gain-frequency curve. This amounts to nothing more than a graphical solution to the general equation, $\frac{C}{R} = \frac{G}{1 + GH}$. Overall loop gain, K_2 X FRS/RS is 23.5 db as measured from Figure 7. The block diagram of Figure 5 can now be simplified further by substitution of the closed loop transfer function for the field current loop.

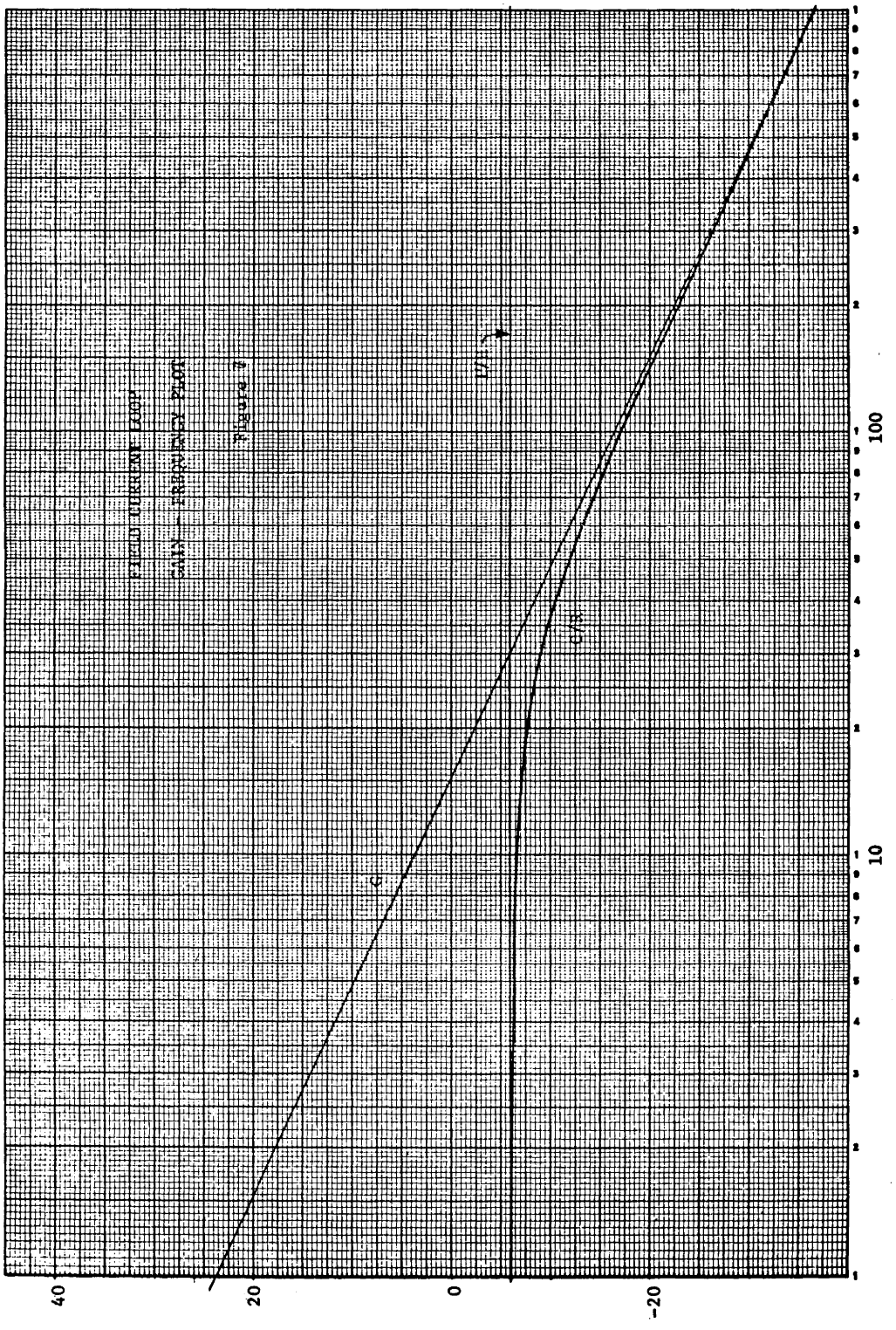
FIELD CURRENT LOOP
GAIN - FREQUENCY PLOT
Figure 7
40
20
0
-20
1
10
100
G
G/R
D/I

Figure 7

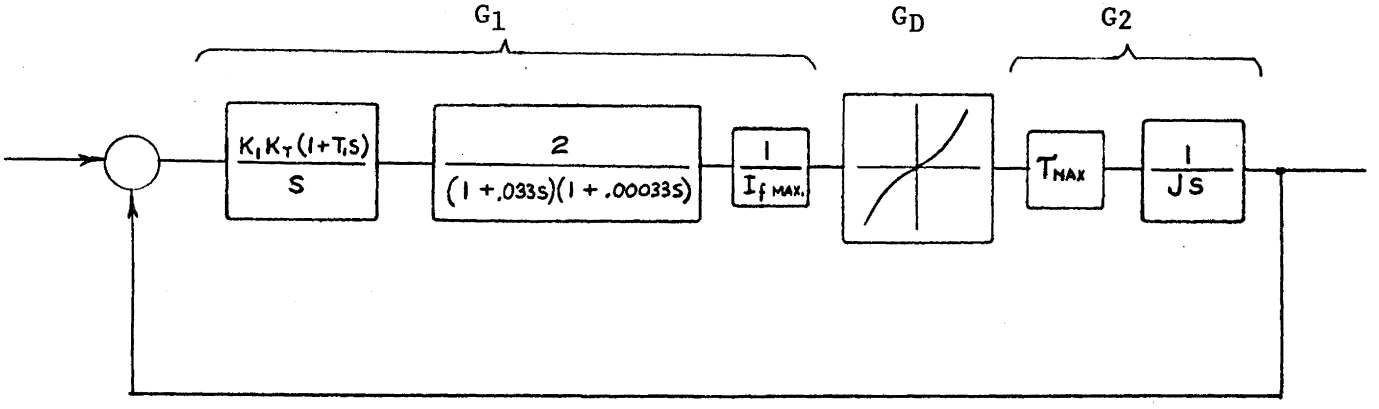

Figure 8

4. Velocity Loop

The gain elements of the reduced block diagram, Figure 8, are grouped as follows for the purpose of isolating linear and nonlinear elements.

G_1 - Tachometer, speed amplifier, field current transfer function, and $1/I_f$ max.

G_2 - T_{max} and $\frac{1}{JS}$

G_D - Absolute square nonlinear element.

The open loop gain is then:

$$GH = G_1 G_D G_2$$

$$G = G_1 G_D G_2 \text{ for } H = 1 \qquad (1)$$

The speed amplifier transfer function,

$$\frac{e_o}{e_{in}} = \frac{K_1 (1 + T_1 S)}{S}$$

is selected for the following reasons:

1. The integration term increases gain prior to unity gain crossover, thus reducing error in that region of frequencies.
2. The lead term is necessary to obtain 20 db per decade attenuation in the vicinity of unity gain crossover. This will reduce error by improving settling time.

The stability analysis is begun by selecting the lead time constant 15 to 1 greater than the time constant after unity-gain crossover. This should insure sufficient damping by creating a substantial 20 db per decade slope in the vicinity of unity gain crossover.

Open loop gain less the describing function:

$$G = G_1 G_2 = K_{Tach} \cdot \frac{K_1 (1 + .2S)}{S} \cdot \frac{2}{(1 + .033S)(1 + .0003S)} \cdot \frac{62.5}{40} \cdot \frac{30}{S}$$

$$G = \frac{K' (1 + .2S)}{S^2 (1 + .033S)(1 + .0003S)} \qquad (2)$$

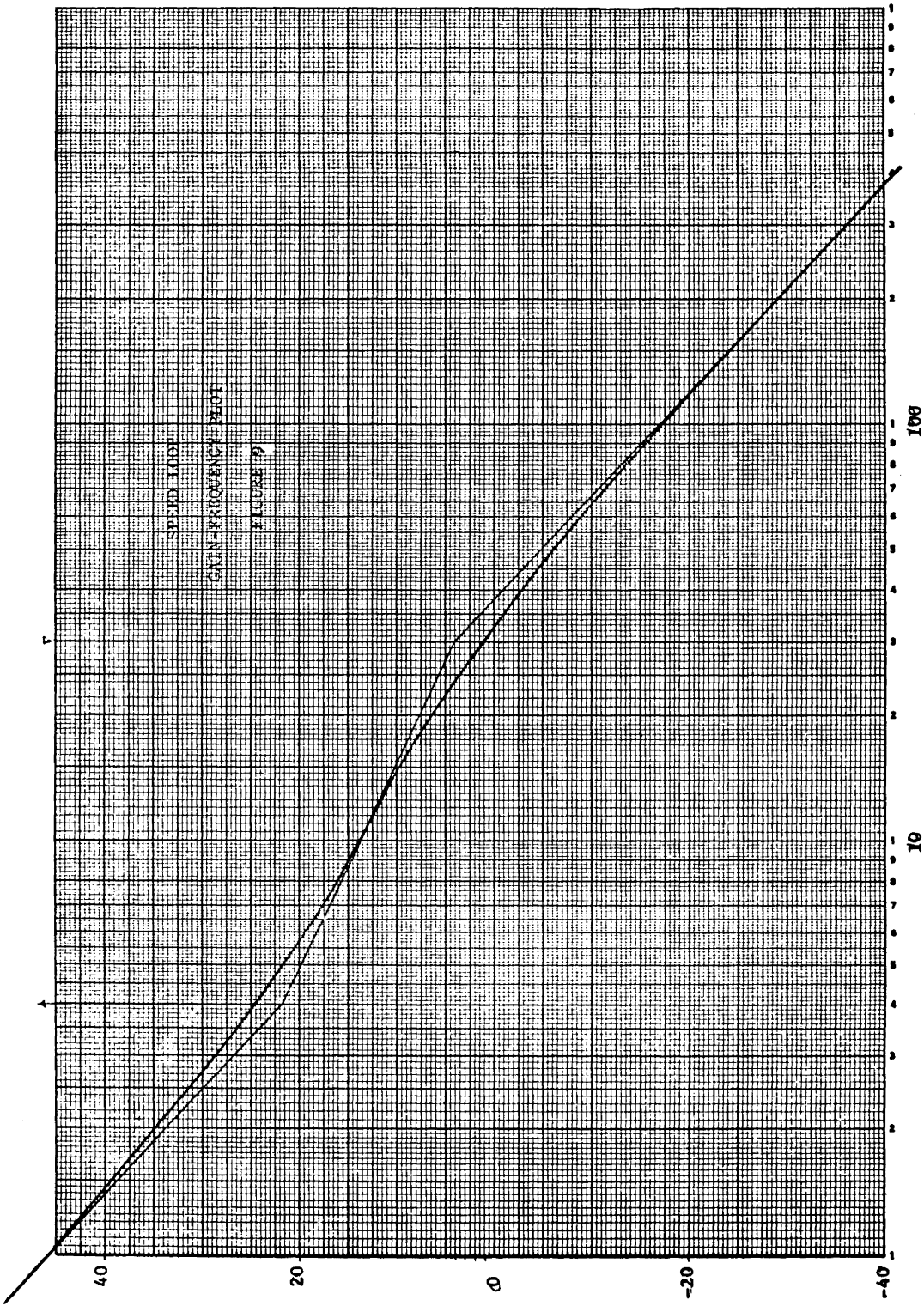

Figure 9

The total open loop gain magnitude K' is set at 200 for a starting point. This value for gain should result in some overshoot, based on a phase shift of 147° at unity gain crossover, which is desirable from the standpoint of defining time-to-peak, settling time, damping ratio, etc. A gain-frequency plot of equation (2) for K' = 200 is shown in Figure 9 page *26*.

5. Describing Function Development

A describing function G_D, is developed for a modified version of the absolute square function. The modified version includes overlap or bias -- a necessary requirement in most push-pull configurations. The development follows basic procedures as described by Thaler and Pastel[7]. To describe this procedure briefly, a gain function expressing the fundamental of the output signal over the input signal is derived allowing a frequency domain analysis to be used. The accuracy of this procedure depends on the output signal harmonic content, its magnitude, and the added attenuation of the harmonics due to system break frequencies beyond that of the fundamental. A describing function for the absolute square function with overlap is developed by first defining the composite curve throughout the region of interest.

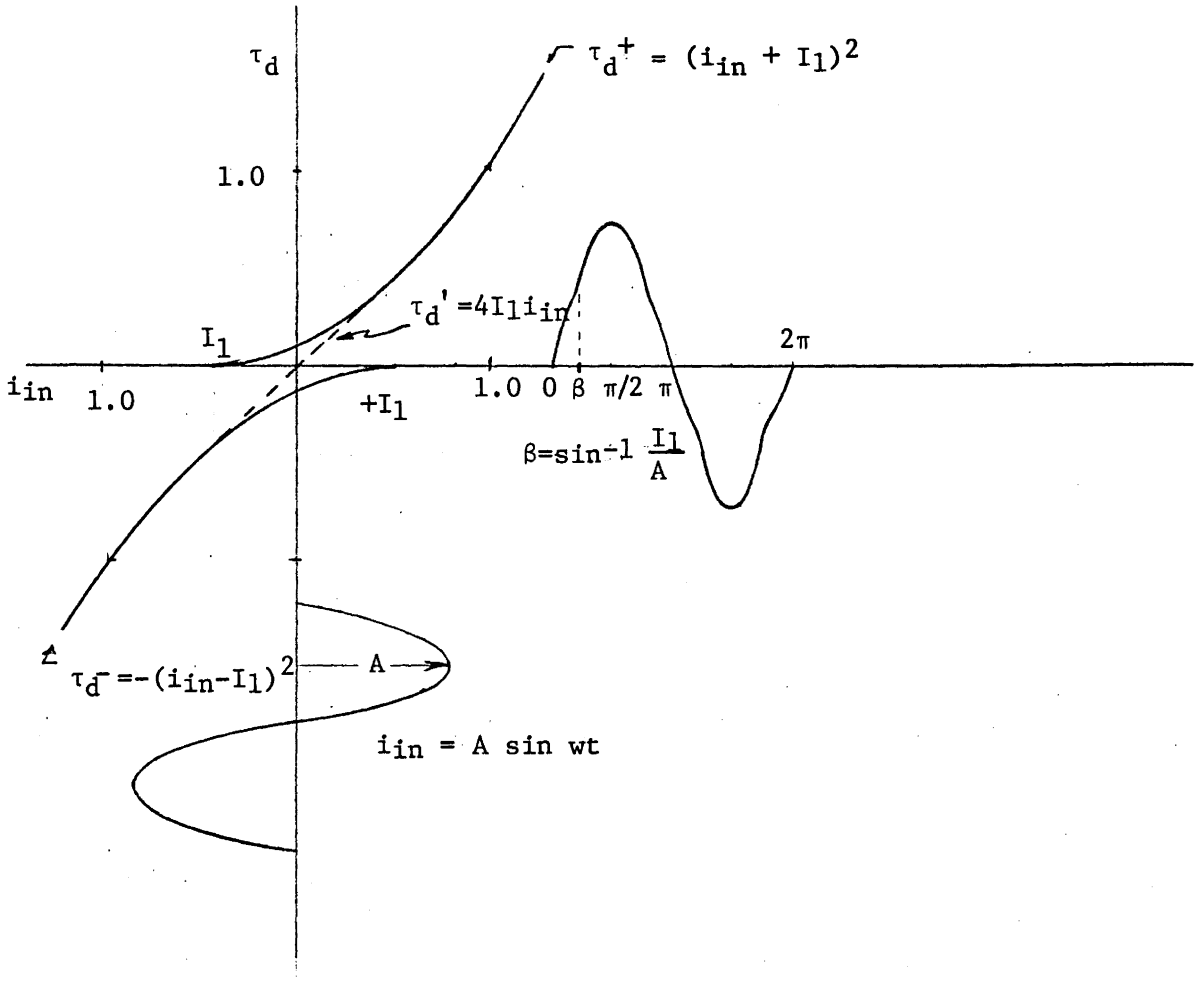

Figure 10

In the region of overlap:

$$\tau_d' = \tau_d^+ + \tau_d^- = i_{in}^2 + 2I_1 i_{in} + I_1^2$$

$$- i_{in}^2 + 2I_1 i_{in} - I_1^2$$

$$\tau_d' = 4I_1 i_{in}$$

Then; $\tau_d = (i_{in} + I_1)^2 \qquad I_1 < i_{in} < 1.0$

$\tau_d = 4I_1\, i_{in} \qquad -I_1 < i_{in} < I_1$

$\tau_d = -(i_{in} - I_1)^2 \qquad -1.0 < i_{in} < -I_1$

The Fourier series for the output wave form τ_d may be written

$$\tau_d(t) = \frac{A_0}{2} + A_1 \cos wt + B_1 \sin wt + A_2 \cos 2wt + B_2 \sin 2wt + \ldots.$$

where the coefficients are given by

$$A_N = \frac{2}{\pi} \int_0^{\pi} \tau_d(t) \cos N\, wt\, dwt$$

$$B_N = \frac{2}{\pi} \int_0^{\pi} \tau_d(t) \sin N\, wt\, dwt$$

Only the fundamental terms will be of interest as discussed previously. Thus the coefficients of interest are A_1 and B_1 which define the fundamental output frequency as

$$\tau_d(t) = \sqrt{A_1^2 + B_1^2} \qquad \underline{/ \tan^{-1} \frac{A_1}{B_1}}$$

A describing function may now be written.

$$G_D(jw) = \frac{\sqrt{A_1^2 + B_1^2} \qquad \underline{/\tan^{-1} \frac{A_1}{B_1}}}{A \qquad \underline{/ 0^\circ}}$$

The output wave form, τ_d possesses 1/4 wave symmetry as shown in Figure 10. Therefore, all even terms are zero, hence $A_1 = 0$.

Then: $G_D(jw) = \dfrac{B_1 \angle 0°}{A \angle 0°}$

$$B_1 = \frac{4}{\pi} \int_0^{\pi/2} \tau_d \sin\theta d\theta \qquad \theta = wt$$

$$B_1 = \frac{4}{\pi} \{\int_0^{\beta} (4I_1 A \sin\theta) \sin\theta d\theta + \int_{\beta}^{\pi/2} (A \sin\theta + I_1)^2 \sin\theta d\theta\}$$

$$B_1 = \frac{4}{\pi} \{\int_0^{\beta} 4I_1 A \sin^2\theta d\theta + \int_{\beta}^{\pi/2} (A^2 \sin^2\theta + 2I_1 A \sin\theta + I_1^2) \sin\theta d\theta\}$$

$$B_1 = \frac{4}{\pi} \{\int_0^{\beta} 4I_1 A \sin^2\theta d\theta + \int_{\beta}^{\pi/2} A^2 \sin^3\theta d\theta + \int_{\beta}^{\pi/2} 2I_1 A \sin^2\theta d\theta + \int_{\beta}^{\pi/2} I_1^2 \sin\theta d\theta\}$$

$$B_1 = \frac{4}{\pi} \{4I_1 A [\frac{\theta}{2} - \frac{\sin 2\theta}{4}]_0^{\beta} + A^2 [\frac{1}{3}\cos^3\theta - \cos\theta]_{\beta}^{\pi/2} + 2I_1 [\frac{\theta}{2} - \frac{\sin 2\theta}{4}]_{\beta}^{\pi/2} - I_1^2 [\cos\theta]_{\beta}^{\pi/2}$$

$$B_1 = \frac{4}{\pi} \{A^2 \ (\cos\beta - \frac{1}{3} \cos^3\beta) + I_1 A \ (\beta + \frac{\pi}{2} - \sin 2\beta) + I_1^2 \cos\beta\}$$

$$G_D(jw) = \frac{B_1 \angle 0°}{A \angle 0°} = \frac{4}{\pi} \{A \ (\cos\beta - \frac{1}{3} \cos^3\beta)$$

$$+ I_1 \ (\beta + \frac{\pi}{2} - \sin 2\beta) + \frac{I_1^2}{A} \cos\beta\}$$

$$\beta = \sin^{-1} \frac{I_1}{E}$$

Let $I_1 = .05$ (5% overlap) in order to retain almost full effect of the absquare nonlinearity while eliminating any backlash in the gearing. Also eliminated is the zero gain slope at the origin -- an undesirable feature in most regulating systems. A plot of the describing function in normalized form is shown in Figure 11.

The describing function approach is straightforward and easy to apply when the nonlinearity is symmetrical about the origin, i.e. no zero-frequency component in its Fourier series. It is not impossible to use otherwise, but more difficulties are encountered. In this analysis, the describing function will operate always about the origin in a symmetrical fashion. This implies no steady-state torque loading will be encountered.

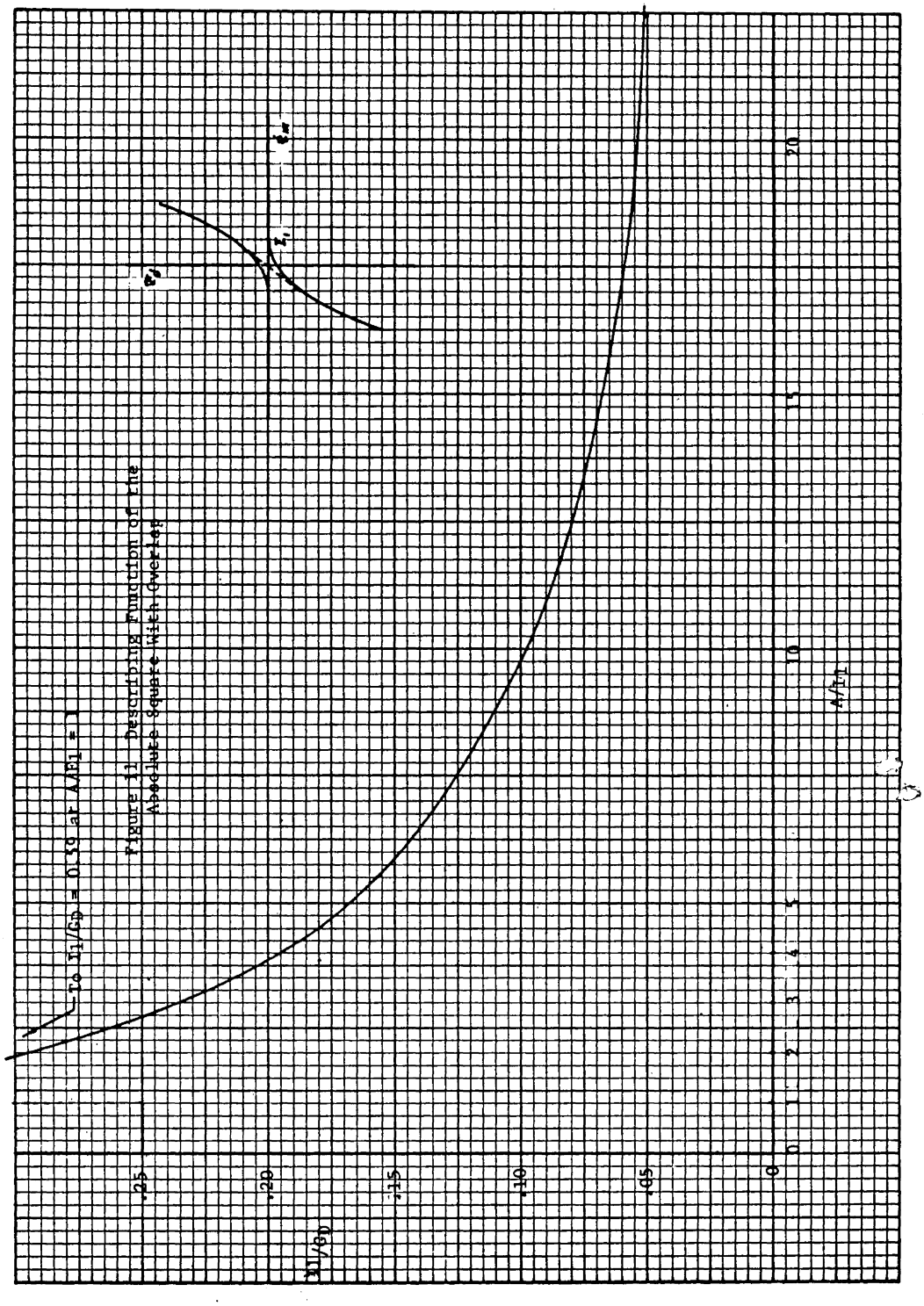
Figure 11 Describing Function of the
Absolute Square With Overlap
To I1/Gp = 0.10 at A/E1 = 1
I1/Gp
.25
.20
.15
.10
.05
0
0 1 2 3 4 5
10
15
20
A/E1
E2'
E2''
E1'
E1''

Figure 11

6. Stability Analysis With The Gain - Phase Shift Plot

From the open loop gain equation, (1), the characteristic equation may be written in the usual form for stability analysis:

$$1 + G_1G_DG_2 = 0$$

$$G_1G_DG_2 = -1$$

$$G_1G_2 = -\frac{1}{G_D} \qquad (3)$$

Equation (3) is plotted on gain-phase shift coordinates for the purpose of estimating transient response with a method suggested by Brearly[7] which utilizes second order linear system criteria as an approximation. Maximum closed loop magnitude, M_m, must be determined for each value of signal input magnitude to the describing function. A transparent Nichol's chart used as an overlay on the $G(j\omega)$, $-\frac{1}{G_D}$ plot facilitates this procedure. See figures 12a and 12b.

The procedure is started by assuming 100% overshoot. For a 1 p.u. excursion, the corresponding amplitude, A, would be two. The origin of the Nichol's chart overlay is placed on this point to determine the intersection of the constant M contours and the $G(j\omega)$ locus. The parameters read at the intersection are: M_m from the M contours and ω_0 from the $G(j\omega)$ locus. This information can be used along with the linear second order equations to correct the

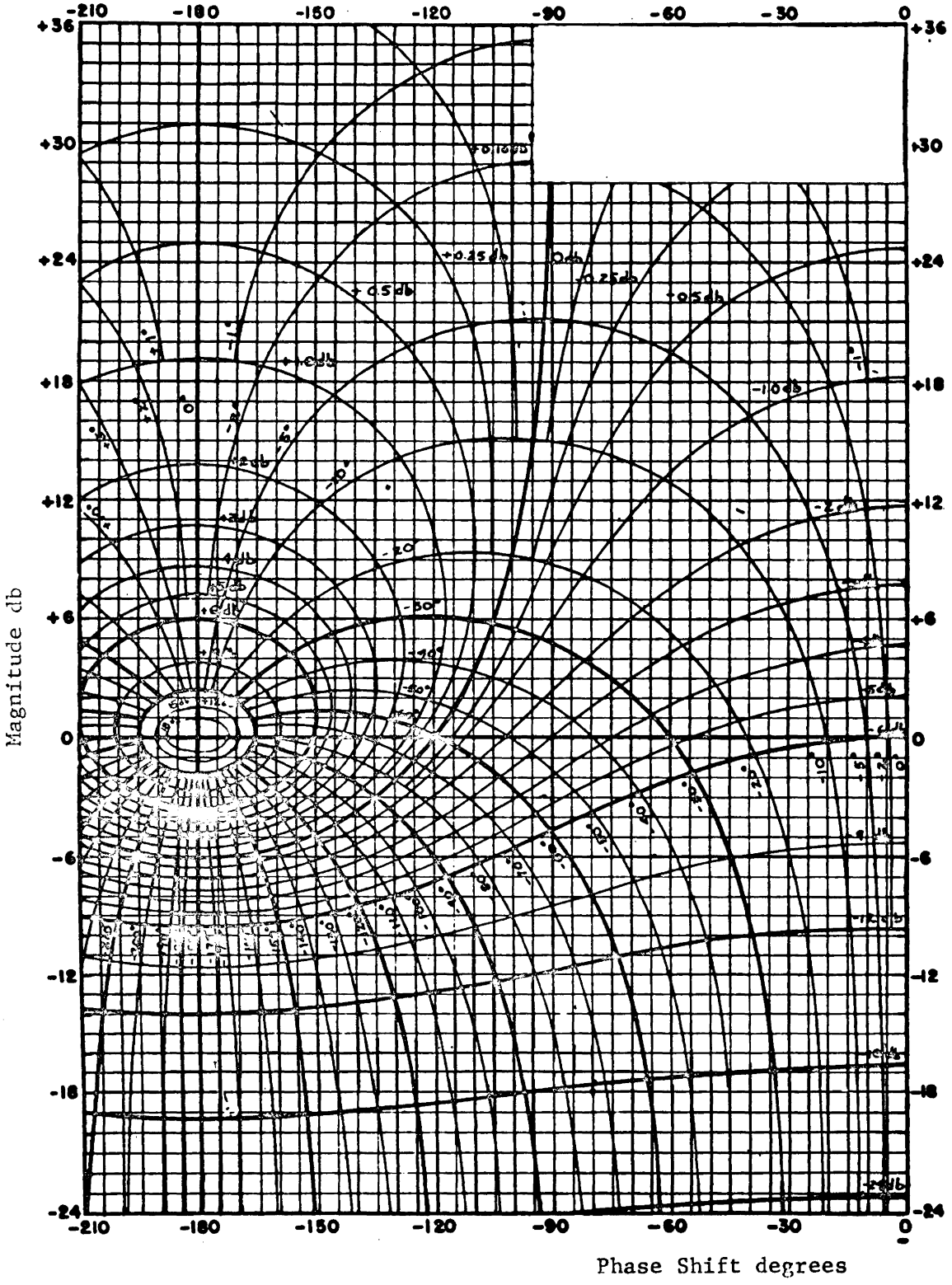

Figure 12a. Nichol's Chart Overlay

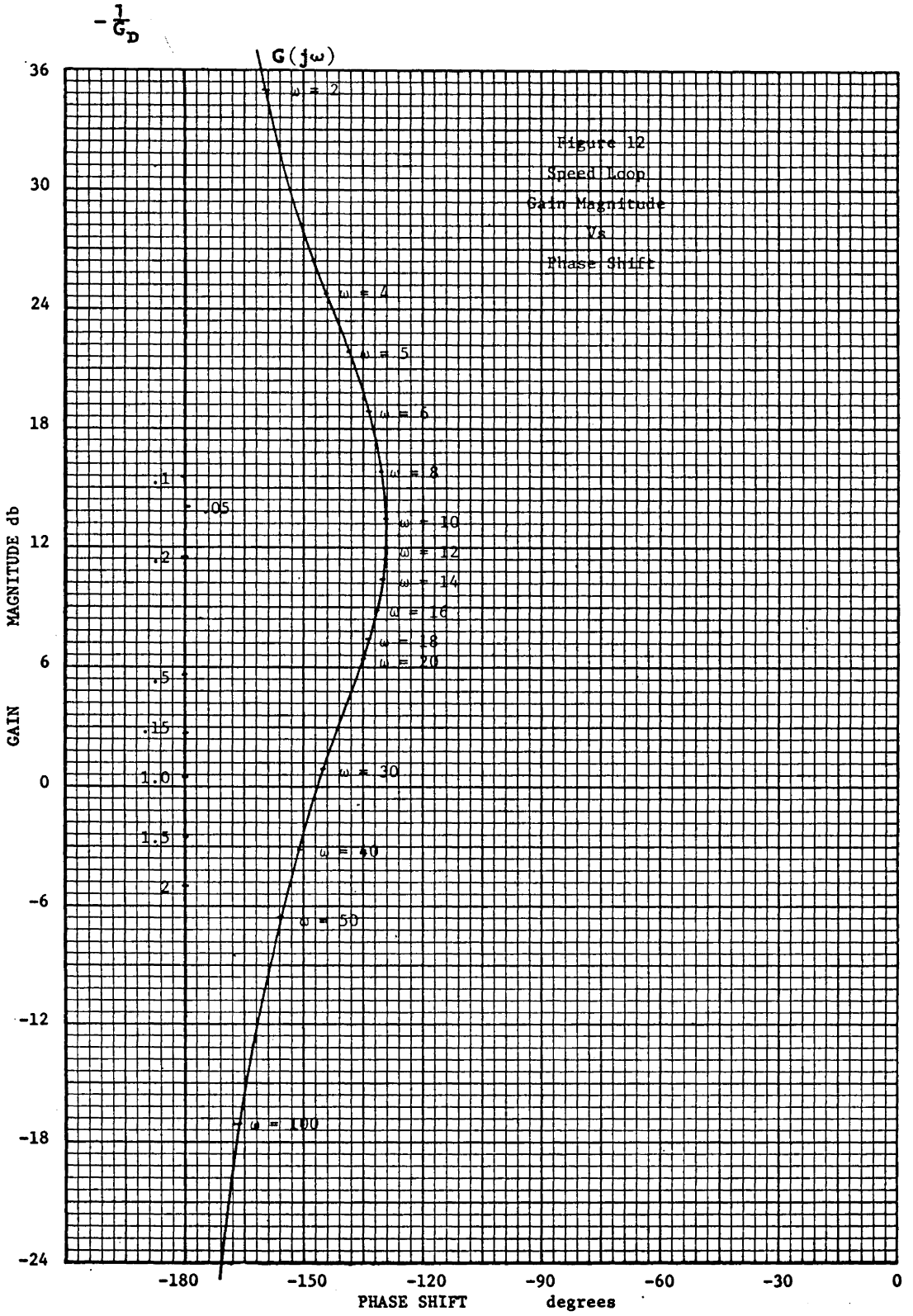

Figure 12b. Gain-Phase Shift Plot

original estimation on overshoot. This process is repeated every half cycle to give the approximate transient response in an iterative fashion.

An example of this method is compared with the analog computer solution in Figure 17.

7. Analog Computer Simulation

The system configuration shown in the block diagram Figure 5 was used for the first computer run. Parameters are the same as those used in the preceding analysis. Data recorded on this run is shown in Figure 15. For the second run, loop gain was reduced and lead time constant T_1 was increased to achieve zero overshoot when subjected to a step input resulting in a 100% torque excursion. Data recorded on this run is shown in Figure 16. The system was then linearized by increasing the absolute squaring function overlap to 100% ($I_1 = 1.0$) and gain was adjusted for the same overshoot when subjected to a step input, resulting in a 100% torque excursion. Data recorded on this run is shown in Figure 18.

Some of the more significant results are tabulated as follows:

		Rise Time, t_r	Settling Time, t_s	Speed Excursion
High Gain $K'=200$ $T_1=0.2$	Linear Sys.	.036 secs.	.276 secs.	80 rpm
	Nonlinear	.024 secs.	.228 secs.	37 rpm
Low Gain $K'=45$ $T_1=2.0$	Linear	.14	.212	210 rpm
	Nonlinear	.07	.136	110 rpm

For those systems which operate with steady state torque load levels ranging from zero to maximum torque, a nonlinear compensation scheme was worked out. A squaring circuit was used in the feedback path of the current loop yielding a square root function in the closed loop transfer function. The product of the square-root gain function and the absquare function is a linear function yielding consistent speed response at any torque level as shown in Figure 19.

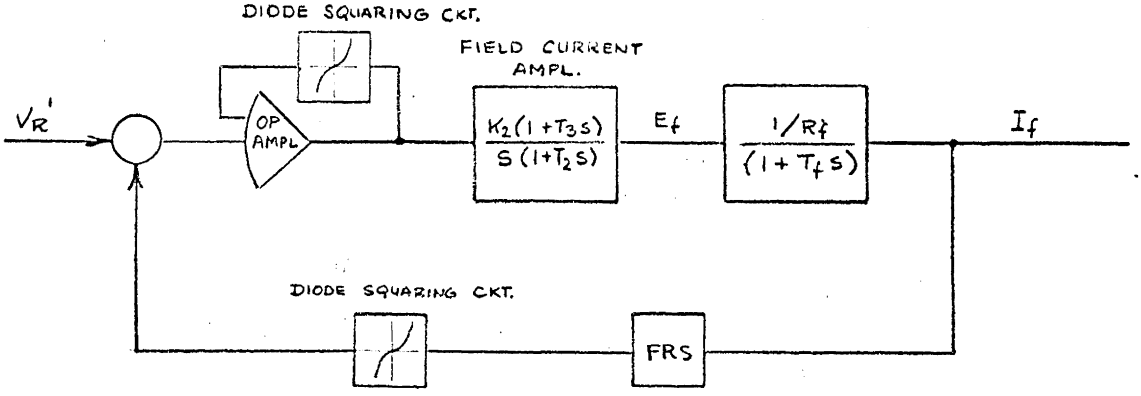

Figure 13. Nonlinear Compensation Scheme

VI. DISCUSSION OF THE RESULTS

The procedure for analyzing eddy-current couplings in feedback control systems as outlined in the analysis should provide a method by which the designer can predict transient performance without being limited to the results obtained from a small signal linearized model.

Results of the analog computer simulation demonstrate how the effects of the nonlinearity can be used to advantage by comparing the nonlinear system with an equivalent linear system. Based on a maximum torque excursion, the nonlinear system is capable of faster response and better damping although the allowable excursion in speed for a maximum torque excursion is only half that of the linear system. Increasing the lead time constant T_1 and decreasing loop gain with K_1 tends to reduce overshoot by the same amount in both the linear and nonlinear systems. Again the response is faster but the excursion in speed is smaller for the nonlinear system based on a maximum torque excursion. Increasing lead and decreasing gain varies the Nichol's chart locus as shown in Figure 14.

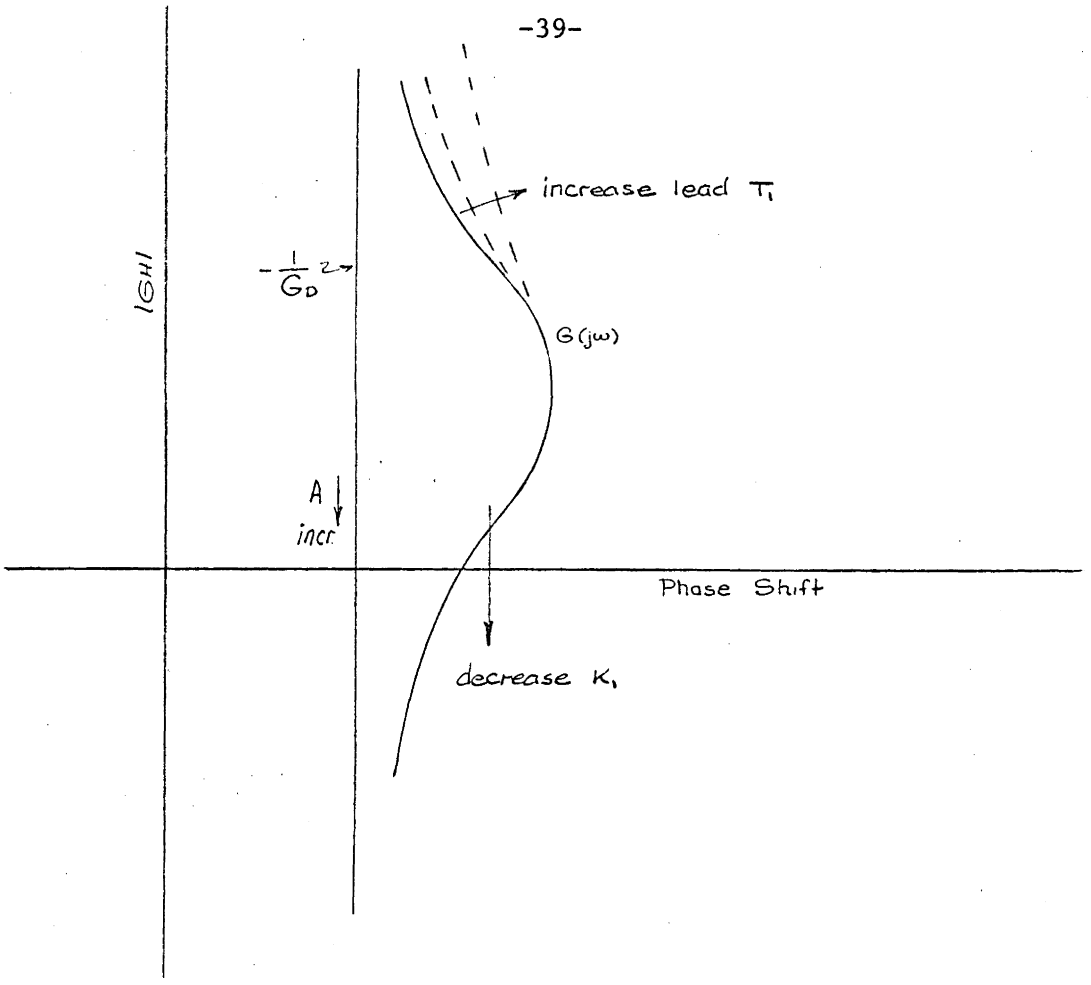

Figure 14

Moving the G(jω) locus away from the $-\frac{1}{G_D}$ locus in the vicinity of A = .05 to A = 1, reduces overshoot, slows response and increases damping.

The design of eddy-current coupling systems with steady state torque loads must follow a somewhat different design procedure. Since the system must operate about any value of torque from zero to maximum torque, system gain varies from 0.2 to 2 for I_1 = .05. The variance in gain is undesirable because the system must be stabilized for the highest value of gain which results in poor response at

lower values of torque. This approach is not very satisfactory, so in the past push-pull couplings have been linearized with a large amount of overlap, resulting in high losses at zero output power. In the development of the describing function, it is shown that as I_1 approaches unity, the composite gain is linear and has a magnitude of four. Nonlinear compensation showed excellent results in the analog computer simulation. The square root gain function was developed in the forward loop of the speed regulator by placing a diode squaring network in the field current regulator feedback. The results of this experiment are shown in Figure 19. The only problem encountered with this method of compensation is the change in field current loop bandwidth with field current operating point. This difficulty can be overcome by utilizing a second squaring circuit in the feedback of an operational amplifier in the forward path of the current loop resulting in overall linear loop gain. This feature has another advantage in the dynamometer application where torque regulation only is required for certain tests. The transference from field current reference to torque will then be a linear function.

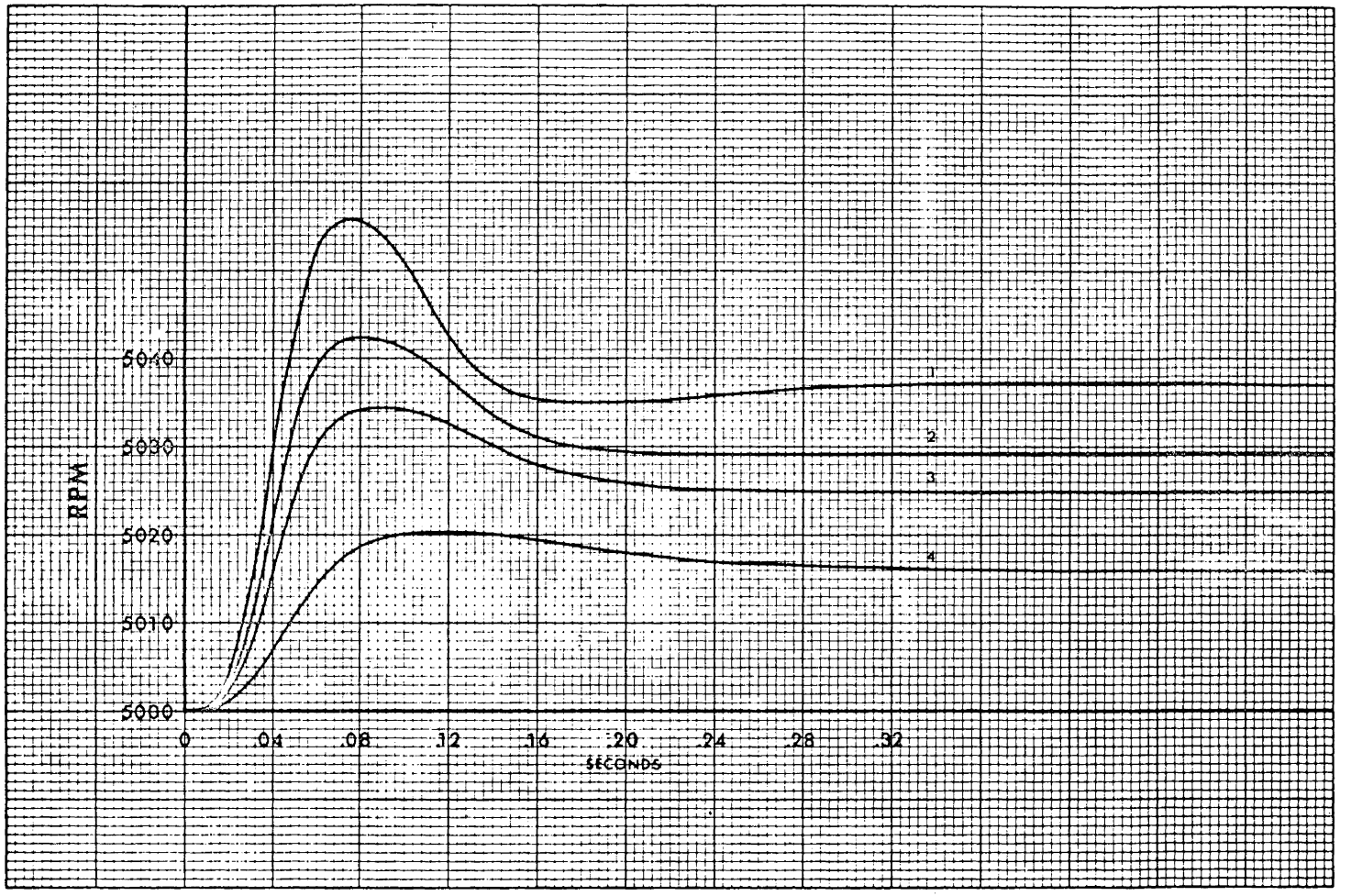

Figure 15, Nonlinear System Speed Response (High Gain)
$K'=200$ $T_1=2$

1. 100% Torque Excursion
2. 75% Torque Excursion
3. 50% Torque Excursion
4. 25% Torque Excursion

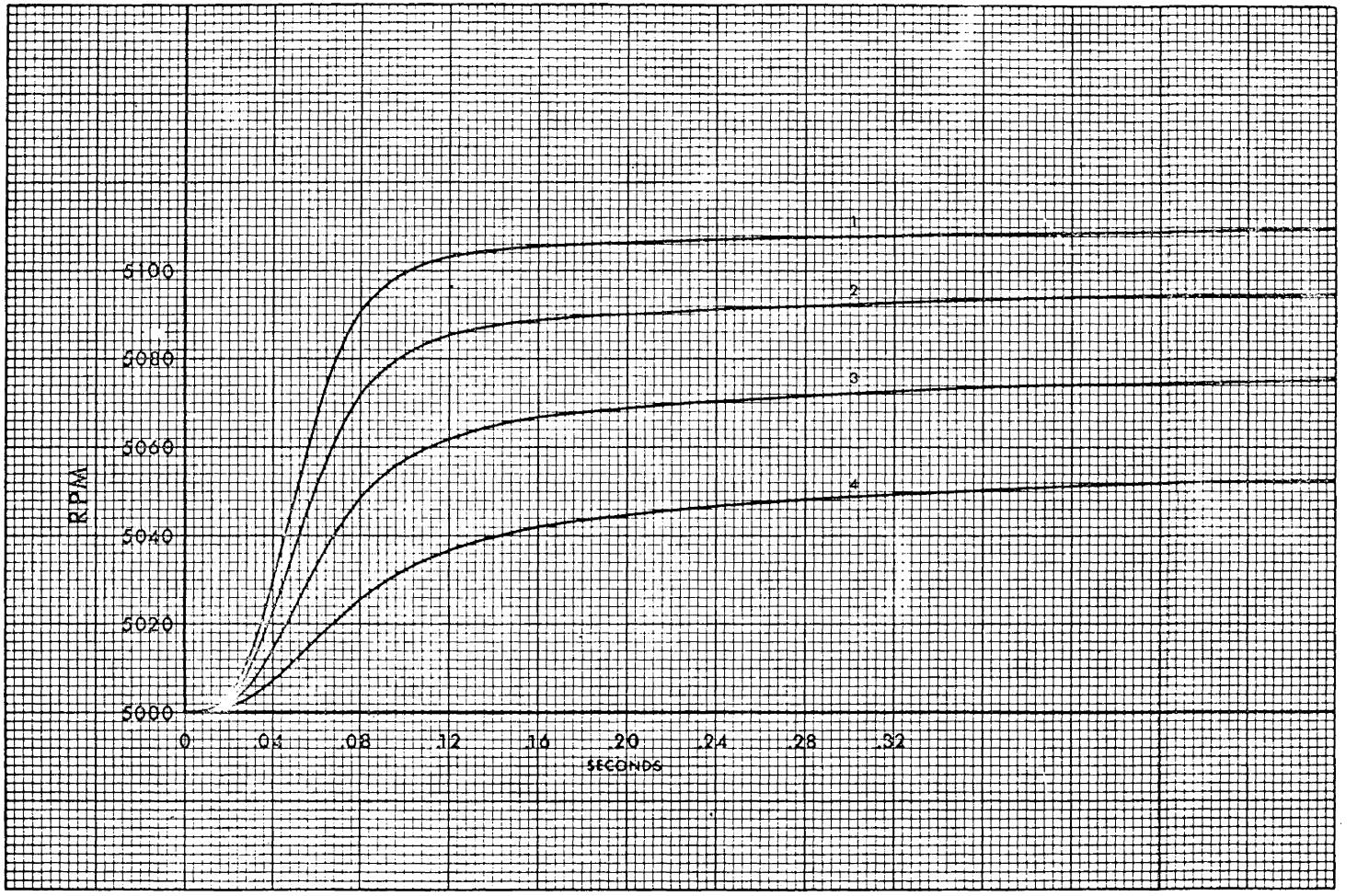

Figure 16. Nonlinear System Speed Response (Low Gain)
$K' = 45$ $T_1 = 2.0$

1. 100% Torque Excursion
2. 75% Torque Excursion
3. 50% Torque Excursion
4. 25% Torque Excursion

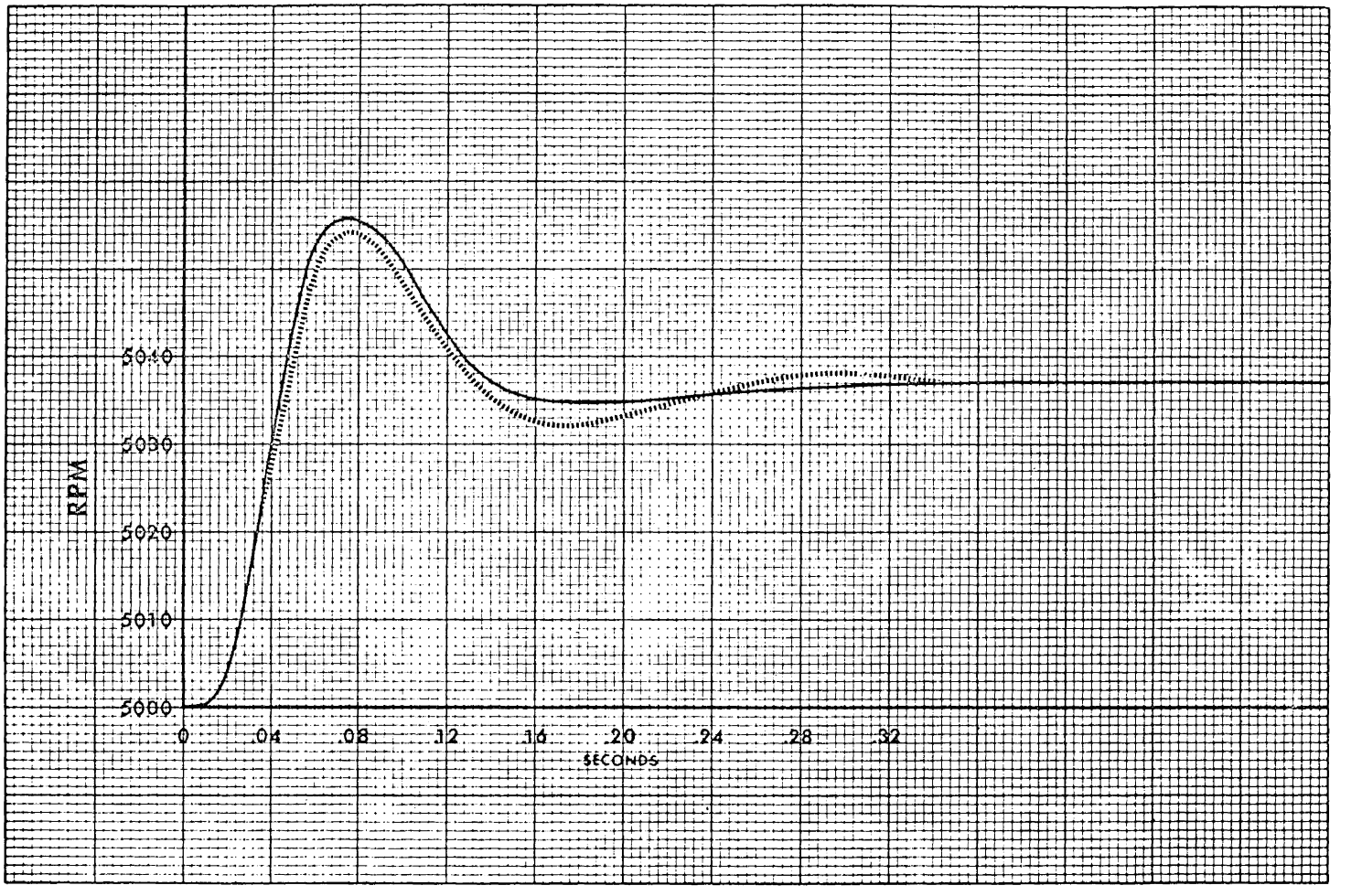

Figure 17. Brearley Approximation and Computer Comparison

——————— Analog Computer

---------- Brearley Approximation (100% Torque Excursion)

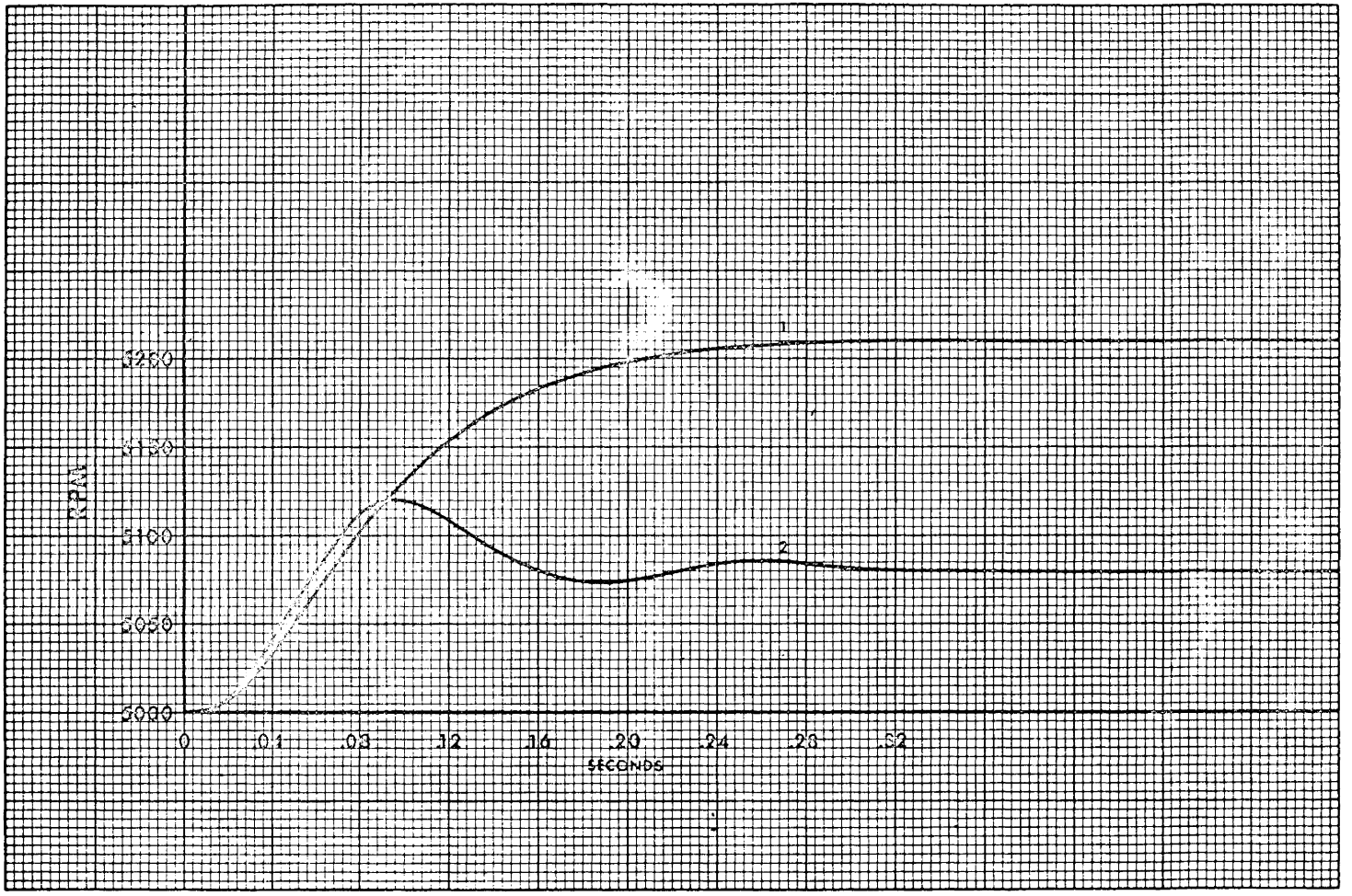

Figure 18. Linear System Speed Response

1. Low Gain 100% Torque Excursion
2. High Gain 100% Torque Excursion

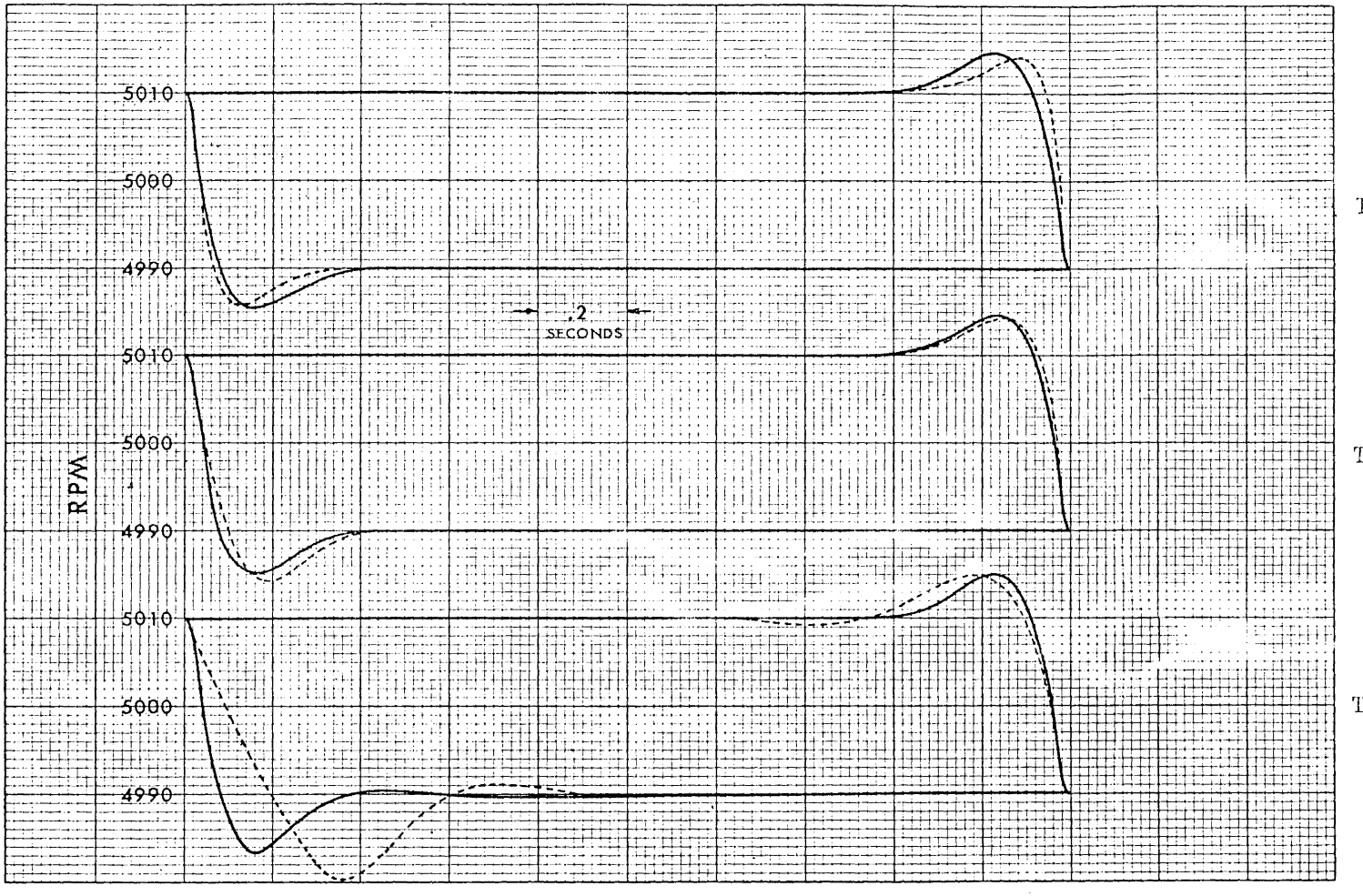

Figure 19. Speed Response at Various Torque Load Levels

——————— With Nonlinear Compensation

---------- Without Nonlinear Compensation

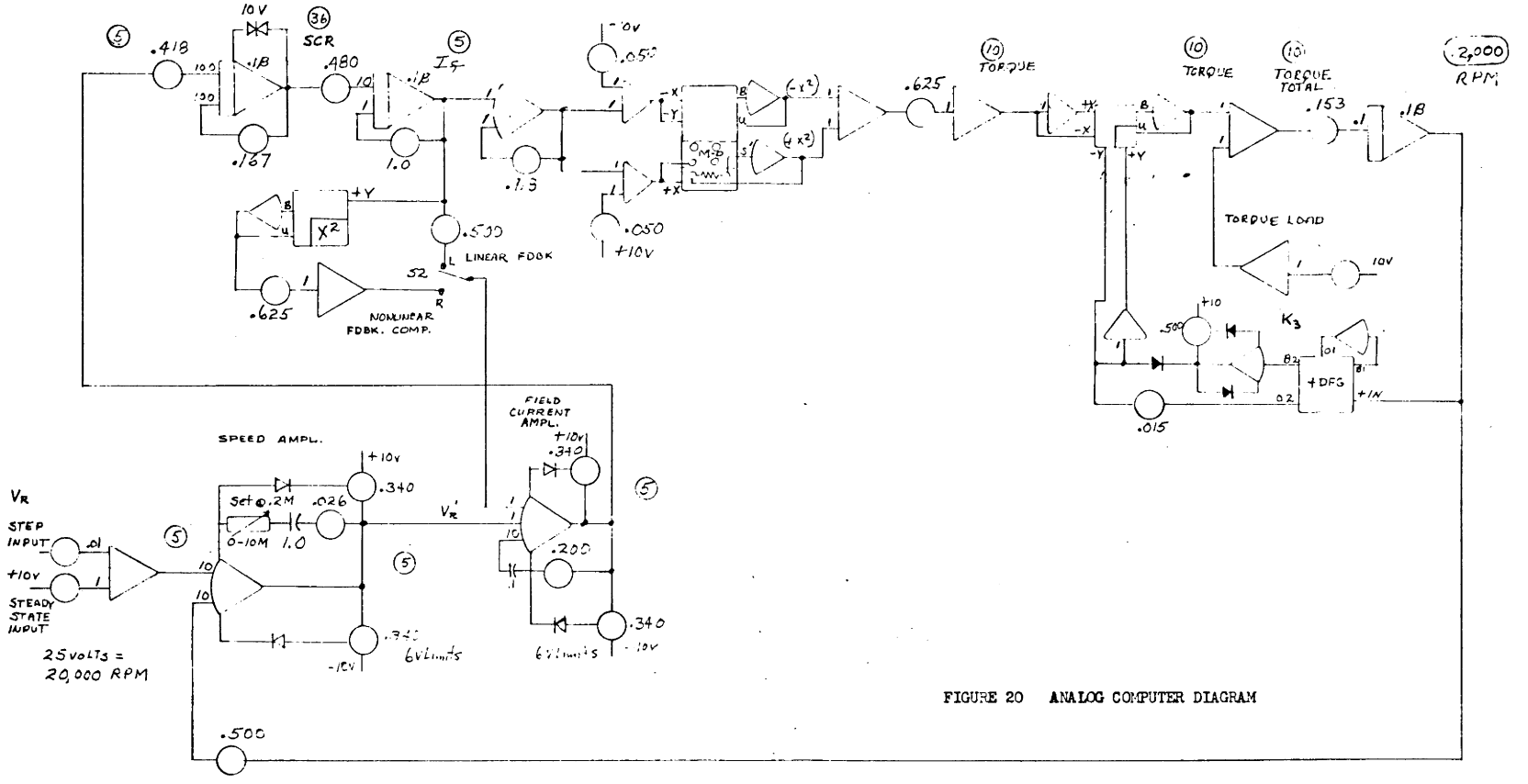

FIGURE 20 ANALOG COMPUTER DIAGRAM

Figure 20

VII. SUMMARY AND CONCLUSIONS

The gain-phase shift plot with Nichol's chart overlay and the describing function developed in the investigation provide a relatively simple method for the estimation of transient response. The method is not only useful in system design, but also very helpful as a check solution in the initial stages of an analog computer simulation where a detailed functional checkout is prone to human error, not to mention component failures. The analog computer is still the most powerful tool for analyzing nonlinear systems, since it can handle higher order systems with more than one nonlinear function and parameters are readily changed or programmed. This statement cannot be made for phase-plane and describing function techniques. On the other hand, the analytical techniques applied to a simplified system result in a better understanding of the system problems.

The absquare nonlinearity can be advantageous in a control system if the load is mainly inertia, so that all torque excursions take place about zero torque. For a given peak torque and percent overshoot, faster rise and settling times are possible at the expense of output excursion magnitude. This feature may be desirable in pulse amplifier design where the absquare nonlinearity could be added or perhaps approximated with a two-slope gain element to improve rise time.

For eddy-current coupling control systems that must operate about various steady-state torque levels, nonlinear gain compensation such as a square root gain function in the forward loop will provide the best solution.

The integration term in the speed amplifier is a very important feature when operating at various torque levels. A change in torque will not affect perfect steady-state speed regulation since zero error is required for constant output. This feature holds true for any offset beyond the speed amplifier.

VIII. ACKNOWLEDGMENTS

The author wishes to express his appreciation to Associate Professor M. H. Hopkins, Jr., his thesis advisor for assistance and suggestions in the preparation of this thesis.

To Mrs. Dorothy Gwaltney must go credit for special care in the typing of this manuscript.

To Ken Stafford for excellent "computermanship" in setting up the Analog Computer and recording the data.

IX. BIBLIOGRAPHY

Literature Cited

1. Gibson, H., "The Eddy Current Inductor Transient Characteristics", General Electric Company Publication IE-1030.321, February 5, 1960.

2. Davies, E. J., "A Study of the Fully-Interdigital Eddy-Current Coupling", General Electric Company Publication No. R61MD707, August 11, 1961.

3. Rudenberg, R., "Transient Performance of Electric Power Systems", McGraw-Hill Book Company, Inc., New York, New York, 1950.

4. Dunaevski, S. I., "Electrichestvo", Moscow, Russia, February 1951, pp. 55-63.

5. Gibbs, W. J., "The Theory and Design of Eddy-Current Slip Couplings", BEAMA Journal, 1946, pages 123-127, 172-177 and 219-225.

6. Volkman, W. K., "Transfer Functions of Eddy Current Couplings", General Electric Company Publication No. DF65MD701.

7. Thaler, G. J. and Pastel, M. P., "Analysis and Design of Nonlinear Feedback Control Systems", McGraw-Hill Book Company, Inc., New York, New York, 1962, pages 181-190.

Literature Examined

1. Chestnut, H. and Mayer, R., "Servomechanisms and Regulating System Design", John Wiley & Sons, Inc., New York, New York, 1951, Volume I.

2. Chestnut, H. and Mayer, R., "Servomechanisms and Regulating System Design", John Wiley & Sons, Inc., New York, New York, 1955, Volume II.

3. Davies, E. J., "A Study of the Fully-Interdigitated Eddy-Current Coupling", General Electric Company Publication No. R61MD707, August 11, 1961.

4. Gibson, H., "The Eddy Current Inductor Transient Characteristics", General Electric Company Publication IE-1030.321, February 5, 1960.

5. Grabbe, E. M, Ramo, S., Wooldridge, D. E., "Handbook of Automation Computation and Control", John Wiley & Sons, Inc., New York, New York, 1958, Volume I.

6. Thaler, G. J., and Pastel, M. P., "Analysis and Design of Nonlinear Feedback Control Systems", McGraw-Hill Book Company, Inc., New York, New York, 1962, pages 181-190.

7. Truxal, J. G., "Automatic Feedback Control Synthesis", McGraw-Hill Book Company, Inc., New York, New York, 1955.

8. Truxal, J. G., "Control Engineers' Handbook", McGraw-Hill Book Company, Inc., New York, New York, 1958.

9. Volkman, W. K., "Transfer Functions of Eddy Current Couplings", General Electric Company Publication No. DF65MD701.

The vita has been removed from the scanned document

NONLINEAR ANALYSIS OF EDDY-CURRENT COUPLINGS IN FEEDBACK CONTROL SYSTEMS

ABSTRACT

A nonlinear analysis is developed for eddy-current couplings in feedback control systems. The analysis makes use of the describing function method to predict transient response.

Effects of the nonlinearity are discussed and backed with an analog computer study. Conclusions arrived at show the absquare nonlinearity to be advantageous under conditions of zero steady state loading or offset.

Under conditions of steady state loading, shifting of the load operating point causes a wide variation in response. This situation is remedied with nonlinear compensation.